JCTC Journal of Chemical Theory and Computation

Article

pubs.acs.org/JCTC

Establishing the Accuracy of Broadly Used Density Functionals in Describing Bulk Properties of Transition Metals

Patanachai Janthon,[†,‡,§,∥] Sergey M. Kozlov,[†] Francesc Viñes,[†] Jumras Limtrakul,[‡,§,∥] and Francesc Illas*[,†]

[†]Departament de Química Física and Institut de Química Teòrica i Computacional (IQTCUB), Universitat de Barcelona, c/Martí i Franquès 1, 08028, Barcelona, Spain

[‡]Department of Chemistry and Center of Nanotechnology, Kasetsart University, Bangkok 10900, Thailand

[§]Center for Advanced Studies in Nanotechnology and Its Applications in Chemical, Food and Agricultural Industries, Kasetsart University, Bangkok 10900, Thailand

[∥]NANOTEC Center for the Design of Nanoscale Materials for Green Nanotechnology Kasetsart University, Bangkok 10900, Thailand

Supporting Information

ABSTRACT: The performance of various commonly used density functionals is established by comparing calculated values of atomic structure data, cohesive energies, and bulk moduli of all transition metals to available experimental data. The functionals explored are the Ceperley–Alder (CA), Vosko–Wilk–Nussair (VWN) implementation of the Local Density Approximation (LDA); the Perdew–Wang (PW91) and Perdew–Burke–Ernzerhof (PBE) forms of the Generalized Gradient Approximation (GGA), and the RPBE and PBEsol modifications of PBE, aimed at better describing adsorption energies and bulk solid lattice properties, respectively. The present systematic study shows that PW91 and PBE consistently provide the smallest differences between the calculated and experimental values. Additional calculations of the (111) surface energy of several face centered cubic (*fcc*) transition metals reveal that LDA produces the most accurate results, while all other functionals significantly underestimate the experimental values. RPBE severely underestimates surface energy, which may be the origin for the reduced surface chemical activity and the better performance of RPBE describing adsorption energies.

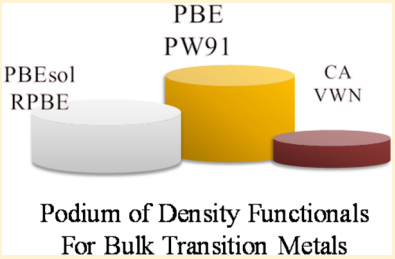

1. INTRODUCTION

Density Functional Theory (DFT) based methods[1,2] are nowadays routinely used in a variety of fields, encompassing quantum chemistry,[3] solid state physics,[4] materials science,[5] and heterogeneous catalysis,[6] just to mention a few. This is due to the nicely balanced accuracy versus computational cost ratio and the increasing improvement of highly parallelized implementations.[7,8] Nevertheless, these methods rely on approximations to the universal, yet unknown, exact exchange-correlation functional, and so, several questions still remain open.[9] Consequently, it is difficult to assess *a priori* which electron density functional is more adequate for a given problem. Usually, the suitability is concluded *a posteriori* after a comparison of test calculations to experimentally available data, and several data sets have been posed for this purpose, mostly focusing on molecular systems.[10−12] Indeed, a systematic evaluation of the accuracy of various density functionals for different systems is of the utmost importance in the field of electronic structure calculations: On the one hand, they guide the users on the choice of a functional to properly describe a particular property, and on the other hand, they assess the developers on detecting what are the main drawbacks of current functionals.

Nowadays, it is well established that hybrid functionals such as the popular Becke–Lee–Yang–Parr (B3LYP)[13] or subsequent improvements, scuh as those developed by Truhlar and co-workers,[11,14] Adamo and Barone,[15] and Scuseria et al.,[16,17] are required to describe molecular systems and their thermochemistry within the chemical accuracy of 1 kcal mol^{-1}. However, the situation in materials science is quite different since calculations on extended periodic systems still often rely on exchange-correlation functionals based either in the Local Density Approximation (LDA) or the Generalized Gradient Approximation (GGA).[1,4,5] The reason is the significantly higher computational cost, compared to LDA or GGA functionals of hybrid density functionals in periodic calculations, especially when using plane wave basis sets, a common choice for periodic systems. Another more fundamental reason is that, while hybrid functionals are essential to reproduce the band gap and electronic structure of oxides,[18−22] manganites,[23] and cuprates,[24−26] they fail in describing metals, which is related to the slow decay of nonlocal Fock exchange with the interelectronic distance.[27] The difficulties hybrid functionals have dealing with transition metals have been very recently pointed out by Tran et al.[28] in their study on the application of the screened hybrid functional YS-PBE0 to bulk Rh, Pd, and Pt. These authors found that this

Received: November 22, 2012
Published: February 19, 2013

   dx.doi.org/10.1021/ct3010326 | J. Chem. Theory Comput. 2013, 9, 1631−1640

hybrid functional incorrectly predicts a ferromagnetic ground state on these metals, in clear contradiction to reality.

An important distinction between molecular and extended systems is the different types and extent of databases used for the calibration of the exchange-correlation potentials. Whereas for isolated systems the studies assessing the performance of various functionals on carefully constructed reference databases are abundant,[11,12,29] on solids these studies are relatively scarce. Moreover, even in the available studies concerning the accuracy of density functional theory based methods in periodic calculations,[27,28,30−58] transition metals are poorly represented although they are crucial components in heterogeneous catalysis and electrochemistry and are of paramount importance in environmental chemistry. In particular, a few transition metal elements concentrate most of the scientific attention, as schematically shown in Figure 1. The majority of the studies

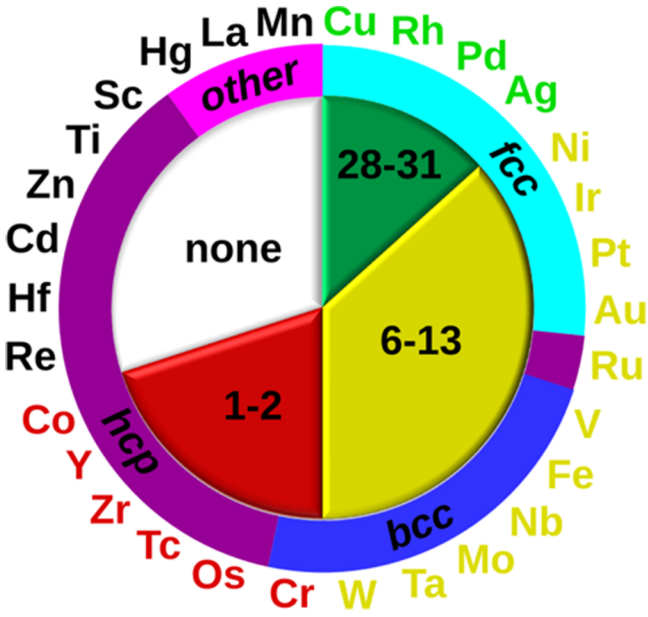

Figure 1. Graphical distribution indicating the number of studies dealing with the accuracy of various exchange correlation functionals on transition metal bulk properties, together with their crystal structure. The distribution is based on 31 references published from 1999 to 2012.[27,30−58] Note that for those metals considered in 1−2 papers, not all of the discussed observables (metal−metal distances, bulk moduli, cohesive energies) have been published.

only focus on Cu, Rh, Pd, and Ag, largely because these elements are often used as benchmarks when developing new exchange-correlation functionals to assess the DFT accuracy.[41,48] Besides, these studies encompass metals with a face centered cubic (*fcc*) crystallographic structure (CS). This is due to the fact that their lattice constants have been experimentally measured near or thermally corrected to 0 K, and relativistic effects for such heavy transition metal elements, though minor, are also known.[59] Thus, it is likely that some of the present density functionals are somewhat biased toward the accurate description of these four transition metals and their particular spatial arrangement, hoping that an equally accurate description will be achieved for the rest of the transition metals, regardless of their crystallographic structure. Interestingly, even Fe, Ni, and Pt, which are very important in industrial catalysis, are often neglected in this type of study. There are more systematic studies dedicated to testing various functionals, although these usually cover only half of the transition metals, mostly sampling, with the caveat of Ru, *fcc* or body centered cubic (*bcc*) structures. There is only one study[50] dealing with a rather broad set containing 19 out of the 30 transition metals and a significant number of *fcc*, *bcc*, and hexagonal closed packed (*hcp*) structures. Unfortunately, even in this study only atomic radii and bulk moduli were examined with various functionals, and hence, some reference data are still missing for Cr, Co, Y, Zr, Tc, and Os. Finally, none of the systematic studies in the literature include Sc, Ti, Mn, Zn, Cd, La, Hf, Re, or Hg in the research scope. All in all, the performance of various density functionals has not been sufficiently studied for half of the transition metal elements of the periodic table. This may lead to significant errors when dealing with these systems due to the different occupation of the d orbitals and to their degree of delocalization, aspects that make each transition metal exhibit its own particular chemistry.

In this work, we assess the performance of ubiquitously used exchange correlation density functionals within LDA and GGA: From LDA, we examined Ceperley−Alder[60] (CA) and Vosko−Wilk−Nussair[61] (VWN) parametrizations and from GGA, the broadly used Perdew−Wang (PW91)[62] and Perdew−Burke−Ernzerhof (PBE)[63] implementations. In addition, we considered the revised version of the PBE (RPBE)[64] functional aimed at providing better chemisorption energies and, furthermore, a revision of PBE designed to provide a better description of lattice properties of solid structures (PBEsol).[47] It should be noted that RPBE was initially proposed on the basis of a few test systems ranging from the adsorption of atomic and molecular oxygen, CO, and NO on Ni(100), Ni(111), Rh(100), Pd(100), and Pd(111) surfaces. Since then, it has been used in a very large number of studies, although none of them focused extensively on the performance of the functional on bulk properties such as metal−metal distances, cohesive energies, and bulk moduli. However, despite the better description of metal−adsorbate interactions, RPBE is thought to yield a poorer description of the binding within a metallic substrate.[49] A similar situation is found for PBEsol, a functional designed to revamp the description of solids by eliminating the bias of PBE toward the description of free atom energies, which is achieved by restoring the first-principles gradient expansion for the exchange part of the functional. The resulting PBEsol was tested for a variety of solids but included Cu, Rh, Pd, and Ag only as representatives of the transition metal series. Despite this, PBEsol is increasingly often chosen for studies involving solids, including transition metals.

The inability to correctly describe both adsorption properties and surface/bulk properties at the same time seems to be a general feature of the broadly used density functional based methods.[49] In spite of the considerations presented above and of the fact that the RPBE and PBEsol versions of the GGA are increasingly used in computational materials science and heterogeneous catalysis studies, it seems necessary to better establish the accuracy of these and other commonly used approaches on a comprehensive series of systems through the simultaneous examination of various properties. In this work, we provide a systematic study of the performance of the above-mentioned LDA and GGA approaches, including also RPBE and PBEsol. The accuracy of these six functionals is established by comparing calculated and experimental results of the interatomic distances, cohesive energies, and bulk moduli of the most stable crystal structure of the 30 transition metal elements in the periodic table. Last but not least, we report

surface related properties for the *fcc* subset of transition metals, and we discuss the effect of the inaccuracy of bulk properties on the surface chemical activity.

2. COMPUTATIONAL DETAILS

DFT calculations have been carried out using the Vienna Ab Initio Simulation Package VASP,[65] employing periodic boundary conditions and sampling CA, VWN, PW91, PBE, RPBE, and PBEsol exchange-correlation functionals. Valence electron density was expanded in a plane-wave basis set with a 415 eV cutoff for the kinetic energy. This ensured variations of total energy below 1 meV with respect to further basis set improvement. Optimizations were performed using the tetrahedron smearing method of Blöchl et al.[66] with an energy width of 0.2 eV to speed up convergence; however, final energy values were corrected to 0 K (no smearing). The effect of the atomic cores into the electron density has been described through the Projector Augmented Wave (PAW) method,[67] using the pseudopotentials recommended in the documentation. Note that scalar relativistic effects may affect bulk properties, especially for heavy elements. These effects are most important in the core electrons, exhibiting very large kinetic energy values, and can be easily incorporated through pseudopotentials, model core potentials, and effective core potential approaches. In the present work, scalar relativistic effects are included through the PAW description of the atomic core region. Previous calculations have shown that explicit inclusion of relativistic effects for the valence electrons of heavy transition metals leads to negligible deviations from present standard PAW approximation, i.e., interatomic distances changes ranging 0.2−0.5 pm and differences in bulk moduli of 3−5 GPa.[59] The electronic structure calculations were non-spin polarized, with the exception of the calculation of isolated metal atoms (in an appropriate box surrounded by a large enough vacuum width) and of magnetic Fe, Ni, and Co bulks. An optimal Monkhorst−Pack[68] grid of 7 × 7 × 7 special **k**-points dimensions was found to be sufficient for accurate total energy calculations in the most stringent metals—those with the smallest unit cell—and so this set has been systematically used for all bulk calculations. Note that energy variations due to the usage of denser **k**-points grids were always below 30 meV. When computing atoms in a vacuum, a broken symmetry cell of 9 × 10 × 11 Å dimensions was employed to ensure proper occupancy of degenerated orbitals. These calculations were carried out at the **Γ** point. Reference atomic values are included in the Supporting Information. In the case of slab calculations, a 7 × 7 × 1 grid was used to sample the reciprocal space. In bulk calculations, ionic positions and cell volumes were optimized using the conjugate gradient algorithm until pressures and total energies were converged within 0.01 GPa and 10 meV, respectively.

Cohesive energies, E_{coh}, were calculated as follows:

$$E_{coh} = E_{at} - \frac{E_{bulk}}{N} \quad (1)$$

where E_{at} is the energy of the isolated metal atom in a vacuum and E_{bulk} is the energy of the bulk unit cell containing N atoms. Within this definition, the larger the positive values of cohesive energies, the stronger is the chemical bonding within the solid. Bulk modulus (B_0) measures the volume variation of the solid (V) due to an external pressure (P), defined as

$$B_0 = -V_0\left(\frac{\partial P}{\partial V}\right)_{T,Vo} \quad (2)$$

where the negative sign shows that volume decreases when a positive external pressure is applied. Variation of the external pressure versus volume is gained via linear regression using the value at equilibrium geometry plus four single point calculations with ±0.05 and ±0.10 Å modifications of the lattice constants. More details of the procedure are detailed elsewhere.[69]

Under normal conditions, most of the 30 transition metals exhibit either *fcc*, *bcc*, or *hcp* crystallographic structures (see the Supporting Information for illustrative pictures). However, there are three exceptions to this: La and solid Hg present hexagonal (h) and rhombohedral (r) unit cells, respectively, and Mn features a cubic unit cell (c) containing 58 atoms, distributed as two Mn_{29} clusters centered in the cell origin and center—thus, similar to a *bcc* structure. In the following, the shortest interatomic distance within a crystal cell, δ, will be compared to the experimental values. However, note that δ depends on the lattice parameter a; in the *fcc* structure, it equals $a/\sqrt{2}$, while for *bcc* it equals $a\sqrt{3}/2$. In the case of *hcp* and h structures, δ depends on two lattice parameters, a and c. In the *hcp* structure, δ may either equal a or $\sqrt{(c^2/4 + a^2/3)}$ depending on the c/a ratio. Finally, for h structures, δ may equal either a or $\sqrt{(c^2/16 + a^2/3)}$, again depending on the c/a ratio, which is always kept constant. In r structures, both δ and a are the same quantity.

Last but not least, in order to connect surface chemical activity with a degree of accuracy in bulk description, we calculated the (111) surface energies of all transition metal elements with the *fcc* crystal structure (Rh, Ir, Ni, Pd, Pt, Cu, Ag, and Au), often encountered as components of heterogeneous catalysts. Surface energies, γ, were derived in two different ways: On one hand, surface energies of either the fixed or relaxed surface can be gained from the relaxation of a six layer slab optimizing the three outermost layers while freezing the remaining ones to the corresponding optimized bulk, following the usual general procedure.[69] A second procedure involves the definition of the slab total energy, E_{slab}, as

$$E_{slab} = N\varepsilon + 2\gamma A \quad (3)$$

where N is the number of atoms composing the slab unit cell, ε is the total energy of each atom in the slab, and A is the surface area of each of the two exposed surfaces. Within this methodology,[70,71] one has to consider a set of slabs with different thicknesses and to perform a linear regression of E_{slab} as a function of N. Surface energy is simply gained from the intercept which equals $2\gamma A$, and the slope gives the bulk energy ε. In the present work, thicknesses from four to nine layers were used for the linear regressions. The linear regression method is able to avoid erroneous results depending on the computational parameters.[72] Also its statistical accuracy can be estimated by 95% confidence intervals.

Due to the large number of studied systems and functionals used, we analyze the results profiting from standard error analysis, i.e., not only Mean Error (ME) but also Mean Absolute Error (MAE), which counteracts possible cancellation of errors in ME. Finally, the Mean Absolute Percentage Error (MAPE) provides the degree of inaccuracy of the functional under study. The MAE, ME, and MAPE values were calculated using standard definitions.

3. RESULTS AND DISCUSSION

The results for the 30 transition metal elements calculated with VWN, PBE, RPBE, and PBEsol exchange-correlation functionals explored in this work are reported in Tables 1−3 for interatomic distances, cohesive energies, and bulk moduli, respectively. The complete sets of calculated data, including CA and PW91 results, are provided in Tables S1−S3 of the Supporting Information. Nevertheless, one must point out that CA and PW91 essentially provided similar results to VWN and PBE exchange-correlation functionals, respectively. Accordingly, CA and PW91 results are not further discussed in detail, and only general trends and significant mean differences are discussed. In the following, we will discuss the sampled functionals performance for each property with the error analysis summarized in Table 4 and graphically displayed in Figure 2. The results concerning surface energies are reported in Table 5 and will be discussed at the end of this section. Nevertheless, one must be aware of the fact that, because of their peculiar crystal structure, results for Mn, La, and Hg will be discussed separately. Including Mn, La, and Hg in the error analysis results in larger deviations and distorts the conclusions, although the relative trends are similar. Finally, we do not compare our results with previous studies in the literature since the main goal here is to establish the accuracy of the six density functionals above-described with respect to experimental data, including all transition metal elements. Nevertheless, it is worth mentioning that the present results follow the trend of those reported in the quite complete study of Ropo et al.[50] and in excellent quantitative agreement with the values reported in the reference paper of Perdew et al.[41] with differences in interatomic distances and cohesive energies with respect to the present values being within 1.2 pm and 0.03 eV, respectively.

Table 1. Calculated and Experimental Shortest Interatomic Distances (δ in pm) of Bulk 3*d*, 4*d*, and 5*d* Transition Metals[a]

element	CS	VWN	PBE	RPBE	PBEsol	exp.
Sc	*hcp*	311.6	321.4	325.7	316.8	325.4[b]
Ti	*hcp*	281.6	288.4	290.8	285.0	289.7[c]
V	*bcc*	251.9	257.7	259.2	254.6	261.3[d]
Cr	*bcc*	241.0	245.9	247.0	243.3	249.8[c]
Mn[e]	*c*	209.0	213.0	215.0	211.0	224.0[f]
Fe	*bcc*	238.5	245.3	247.5	241.6	246.0[g]
Co	*hcp*	240.1	247.0	249.4	243.3	249.7[c]
Ni	*fcc*	242.1	248.9	251.2	244.6	249.3[h]
Cu	*fcc*	249.0	256.7	259.8	252.2	255.6[d]
Zn	*hcp*	278.0	289.0	294.2	281.8	291.3[c]
Y	*hcp*	344.1	354.3	358.5	348.8	355.6[c]
Zr	*hcp*	314.7	319.7	321.3	316.2	317.9[c]
Nb	*bcc*	281.9	287.3	288.6	284.0	285.9[i]
Mo	*bcc*	271.0	274.9	275.8	272.3	272.5[j]
Tc	*hcp*	268.3	272.2	272.7	269.6	271.0[k]
Ru	*hcp*	261.5	265.8	266.6	263.0	265.0[c]
Rh	*fcc*	266.4	271.7	272.9	268.2	253.9[l]
Pd	*fcc*	272.4	279.4	281.6	274.8	275.3[m]
Ag	*fcc*	283.8	294.1	298.1	287.6	288.9[n]
Cd	*hcp*	315.4	330.6	339.5	320.7	329.4[c]
La	*h*	354.5	372.0	378.0	360.9	373.9[c]
Hf	*hcp*	305.7	313.9	315.7	309.7	313.1[c]
Ta	*bcc*	281.8	287.5	288.6	284.2	286.0[c]
W	*bcc*	271.5	275.1	275.4	272.7	274.1[o]
Re	*hcp*	272.1	275.5	275.8	273.2	256.7[p]
Os	*hcp*	265.7	269.4	270.0	267.1	267.5[c]
Ir	*fcc*	270.0	274.1	274.8	271.4	271.5[c]
Pt	*fcc*	276.2	281.1	282.2	277.6	277.2[q]
Au	*fcc*	287.2	295.0	297.5	289.8	287.9[n]
Hg	*r*	309.8	353.2	397.5	321.8	301.0[k]

[a]CS stands for crystal structure (*hcp*, hexagonal close packed; *fcc*, face centered cubic; *bcc*, body centered cubic; *c*, cubic; *h*, hexagonal; *r*, rhombic). [b]Ref 74. [c]Ref 75. [d]Ref 76. [e]Due to the complex unit cell, only the shortest Mn−Mn distance is reported. [f]Ref 77. [g]Ref 78. [h]Ref 79. [i]Ref 80. [j]Ref 81. [k]Ref 82. [l]Ref 83. [m]Ref 84. [n]Ref 85. [o]Ref 86. [p]Ref 87. [q]Ref 88.

Table 2. Calculated and Experimental Cohesive Energies (E_{coh} in eV/atom) of Bulk 3*d*, 4*d*, and 5*d* Transition Metals

element	CS	VWN	PBE	RPBE	PBEsol	exp.[a]
Sc	*hcp*	4.86	4.12	3.72	4.52	3.90
Ti	*hcp*	6.37	5.45	4.96	6.06	4.84
V	*bcc*	7.36	6.03	5.39	6.73	5.30
Cr	*bcc*	5.51	4.00	3.39	4.65	4.09
Mn	*c*	5.42	3.86	3.38	4.61	2.92
Fe	*bcc*	6.41	4.87	4.24	5.61	4.28
Co	*hcp*	6.61	5.27	4.49	5.86	4.43
Ni	*fcc*	6.04	4.87	4.22	5.53	4.44
Cu	*fcc*	4.50	3.48	3.12	4.03	3.48
Zn	*hcp*	1.90	1.12	0.75	1.59	1.35
Y	*hcp*	4.87	4.13	3.75	4.56	4.39
Zr	*hcp*	7.34	6.16	6.27	6.94	6.29
Nb	*bcc*	8.46	6.98	6.39	7.68	7.44
Mo	*bcc*	7.95	6.21	5.57	7.01	6.80
Tc	*hcp*	8.70	6.85	6.17	7.82	7.13
Ru	*hcp*	8.68	6.67	5.92	7.69	6.74
Rh	*fcc*	7.55	5.62	5.19	6.81	5.72
Pd	*fcc*	5.02	3.71	3.09	4.43	3.90
Ag	*fcc*	3.60	2.49	1.98	3.03	2.94
Cd	*hcp*	1.53	0.73	0.33	1.20	1.16
La	*h*	5.09	4.18	3.70	4.72	4.47
Hf	*hcp*	7.53	6.40	5.90	7.07	6.42
Ta	*bcc*	9.63	8.27	7.66	9.09	8.09
W	*bcc*	10.57	9.07	8.42	9.96	8.79
Re	*hcp*	9.61	7.82	7.09	8.79	8.02
Os	*hcp*	10.21	8.29	7.56	9.40	8.17
Ir	*fcc*	9.22	7.32	6.63	8.42	6.92
Pt	*fcc*	7.13	5.50	4.83	6.41	5.85
Au	*fcc*	4.27	2.99	2.40	3.66	3.81
Hg	*r*	0.93	0.15	0.49	0.51	0.62

[a]Ref 90.

3.A. Interatomic Distances. We begin the discussion by comparing the shortest interatomic distances δ of the transition metals calculated with different functionals, compared to the available experimental values, see Table 1. Most recent experimental crystallographic interatomic distances have been collected via the Crystallographic Open Database,[73] and the original sources are also included in the reference list for completeness.[74−88] Note that in general terms the experimental interatomic distances suffer from measurement error bars below ±0.03 pm, and so below the order of magnitude of the significant figures here discussed. Only in a few cases are the experimental bond length error bars on the same order, with Re being the case displaying the worst precision.[87] Nevertheless, for Re the error bars are of ±0.46 pm and, as shown afterwards,

dx.doi.org/10.1021/ct3010326 | J. Chem. Theory Comput. 2013, 9, 1631−1640

Table 3. Calculated and Experimental Bulk Moduli (B_0 in GPa) of Bulk 3*d*, 4*d*, and 5*d* Transition Metals

element	CS	VWN	PBE	RPBE	PBEsol	exp.[a]
Sc	*hcp*	62.9	55.0	51.2	57.9	54.6
Ti	*hcp*	129.4	113.5	103.8	120.7	106.0
V	*bcc*	219.4	183.1	175.0	200.1	155.0
Cr	*bcc*	302.0	261.2	237.6	284.5	160.0
Mn	*c*	333.7	281.9	264.2	311.2	90.4
Fe	*bcc*	256.9	195.3	159.1	216.1	163.0
Co	*hcp*	270.1	212.5	189.0	238.3	186.0
Ni	*fcc*	254.7	193.9	173.2	233.6	179.0
Cu	*fcc*	188.2	146.9	122.3	165.2	133.0
Zn	*hcp*	107.3	78.4	66.4	96.2	64.8
Y	*hcp*	44.2	40.7	38.6	42.6	41.0
Zr	*hcp*	102.6	95.5	92.9	104.2	94.9
Nb	*bcc*	173.8	171.1	164.7	183.5	169.0
Mo	*bcc*	296.8	261.3	254.2	288.9	261.0
Tc	*hcp*	349.6	307.6	294.8	333.8	297.0
Ru	*hcp*	365.2	308.2	295.7	349.1	303.0
Rh	*fcc*	317.7	256.4	238.1	290.8	282.0
Pd	*fcc*	215.6	169.4	151.2	203.8	189.0
Ag	*fcc*	138.7	83.3	74.6	117.4	98.8
Cd	*hcp*	79.7	49.6	39.1	68.9	49.8
La	*h*	30.6	25.1	23.1	27.8	26.6
Hf	*hcp*	124.6	108.0	104.3	114.3	108.0
Ta	*bcc*	213.7	195.3	188.3	209.2	191.0
W	*bcc*	351.7	316.2	306.1	334.8	308.0
Re	*hcp*	415.8	372.1	363.6	405.6	360.0
Os	*hcp*	254.5	402.6	388.4	439.2	418.0
Ir	*fcc*	406.1	347.3	333.4	387.8	358.0
Pt	*fcc*	309.4	250.9	233.5	291.7	277.0
Au	*fcc*	187.2	138.4	120.7	171.9	166.0
Hg	*r*	45.3	9.7	1.9	20.0	28.2

[a]Ref 90.

well below the differences of accuracy of different types of exchange-correlation functionals explored in the present work. Experimental data are chosen whenever possible at temperatures close or extrapolated to 0 K. Nevertheless, transition metal thermal expansion coefficients are on the order of $\sim 10^{-5}$ K^{-1}, and so lattice constant expansions at room temperature would systematically decrease the experimental values of interatomic distances, but not significantly enough to affect the conclusions of this study. Last but not least, a recent study has shown that inclusion of zero-point anharmonic phonon correction on lattice constants little reduces the error statistics of density functionals, by 0.1−0.2% in transition metals.[32]

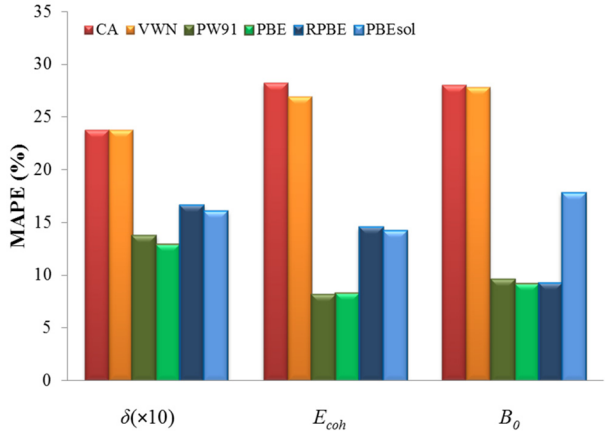

Figure 2. Summary of Mean Absolute Percentage Error (MAPE) for the interatomic distances, δ; cohesive energies, E_{coh}; and bulk moduli, B_0, of the 3d, 4d, and 5d transition metals series excluding metals with particular crystallographic structure: Mn, La, and Hg. MAPE in δ has been multiplied by a factor of 10 for a better visualization.

From the error analysis in Table 4, restricted to the 27 transition metal elements obtained by excluding Mn, La, and Hg, it seems clear that the PBE provides the most accurate description of the atomic structure of bulk transition metals closely followed by PW91. This result is already somewhat surprising because it contradicts the common belief, mostly from molecular systems and organometallic chemistry,[89] that LDA yields significantly better interatomic distances than GGA functionals of broad applicability such as PW91 and PBE. We find that this is the case only for Mo, Rh, Pd, Re, Ir, Pt, and Au (also for Hg). However, when considering the set of 27 transition metals, one can clearly see that GGA performs better. In fact, the MAE of PBE and PW91 functionals for the optimized interatomic distances is of ∼3.5−3.7 pm only, whereas it is considerably larger (∼6.7 pm) in the case of both CA and VWN parametrizations of LDA. Nevertheless, the mean (signed) average error (ME) of interatomic distances for the complete set of 27 transition metal elements corresponding to PW91 and PBE is of only 1.95 and 2.01 pm, respectively. As expected, LDA underestimates all of the interatomic distances (27 transition metals set) by 4.6 pm on average as expected from the well-known tendency of LDA to overestimate binding interactions.

The PBEsol functional designed to reproduce experimental distances between metal atoms in the bulk[47] yields the most accurate results for 6 out of 27 (even 30) transition metal

Table 4. Error Analysis of the Results Corresponding to the Interatomic Distance (δ in pm except for MAPE), Cohesive Energy (E_{coh} in eV atom^{-1} except for MAPE), and Bulk Modulus (B_0 in GPa except for MAPE) of Bulk 3d, 4d, and 5d Transition Metals Excluding Mn, La, and Hg (See Text)

property		CA	VWN	PW91	PBE	RPBE	PBEsol
δ	ME	−4.60	−4.59	1.95	2.01	4.19	−1.98
	MAE	6.67	6.66	3.72	3.49	4.56	4.42
	MAPE	2.38	2.38	1.37	1.29	1.66	1.60
E_{coh}	ME	1.44	1.36	0.02	−0.01	−0.57	0.74
	MAE	1.44	1.36	0.33	0.34	0.59	0.75
	MAPE	28.24	26.94	8.11	8.29	14.49	14.16
B_0	ME	36.12	35.74	7.46	5.21	−7.89	28.79
	MAE	48.23	47.85	16.13	15.66	15.73	28.79
	MAPE	28.06	27.84	9.57	9.17	9.21	17.72

dx.doi.org/10.1021/ct3010326 | J. Chem. Theory Comput. 2013, 9, 1631−1640

Table 5. Surface Energies (in J m^{-2}) Calculated with Various Functionals and Using Either Direct Calculation (dc) or Calculated through Linear Regression (lr)[a]

	CA		VWN		PW91		PBE		RPBE		PBEsol		exp.[b]
	dc	lr	dc	lr	dc	lr	dc	lr	dc	lr	dc	lr	
Ni	2.56	2.48 ± 0.05	2.55	2.48 ± 0.05	1.92	1.89 ± 0.05	1.93	1.92 ± 0.06	1.68	1.65 ± 0.08	2.32	2.28 ± 0.05	2.45
Cu	1.83	1.74 ± 0.17	1.83	1.74 ± 0.17	1.30	1.29 ± 0.11	1.31	1.30 ± 0.11	1.07	1.09 ± 0.10	1.65	1.59 ± 0.17	1.83
Rh	2.53	2.57 ± 0.14	2.53	2.57 ± 0.14	1.94	1.97 ± 0.12	1.94	1.98 ± 0.12	1.72	1.75 ± 0.11	2.42	2.37 ± 0.14	2.70
Pd	1.81	1.79 ± 0.07	1.81	1.79 ± 0.07	1.25	1.27 ± 0.05	1.25	1.27 ± 0.04	1.02	1.05 ± 0.03	1.60	1.60 ± 0.05	2.05
Ag	1.18	1.16 ± 0.03	1.18	1.16 ± 0.03	0.74	0.75 ± 0.03	0.73	0.74 ± 0.03	0.52	0.55 ± 0.02	1.01	1.00 ± 0.03	1.25
Ir	2.81	2.83 ± 0.10	2.81	2.83 ± 0.10	2.25	2.27 ± 0.11	2.27	2.27 ± 0.10	2.06	2.07 ± 0.09	2.65	2.67 ± 0.10	3.00
Pt	1.96	1.95 ± 0.10	1.96	1.95 ± 0.10	1.45	1.44 ± 0.07	1.52	1.46 ± 0.08	1.24	1.25 ± 0.07	1.54	1.80 ± 0.10	2.48
Au	1.19	1.16 ± 0.11	1.19	1.16 ± 0.11	0.74	0.73 ± 0.09	0.74	0.73 ± 0.09	0.54	0.54 ± 0.08	1.02	1.00 ± 0.11	1.50
ME	−0.17	−0.20	−0.17	−0.20	−0.71	−0.71	−0.70	−0.70	−0.93	−0.91	−0.38	−0.37	
MAE	0.20	0.21	0.20	0.21	0.71	0.71	0.70	0.70	0.93	0.91	0.38	0.37	
MAPE	9.55	10.07	9.50	10.07	34.52	34.38	34.00	34.11	45.34	44.71	18.50	18.25	

[a]ME and MAE are in J m^{-2}, whereas MAPE is in %. [b]Ref 91.

elements (Mo, Pd, Ag, Os, Ir, and Pt), whereas, at the same time, the accuracy of the calculated distances for 14 elements (Ni, Fe, Cu, Zn, Y, Zr, Nb, Tc, Ru, Cd, La, Hf, Ta, and W) is clearly inferior to that of PW91 or PBE. A closer inspection of the data in Table 1 reveals that PBEsol improves the PBE parent functional for *fcc* metals only (see deviation analysis for different CSs in the Supporting Information), while its performance is similar for *hcp* and clearly worse for *bcc* metals. Note that PBEsol was developed considering Cu, Rh, Ag, and Pd, all exhibiting *fcc* structure. This provides one more indication of the need to consider a sufficiently broad number of cases when designing and testing new functionals. From the accuracy analysis in Table 4, one finds that, regarding interatomic distances, the MAE of PBEsol is 4.42 pm, which is somewhat higher than those of PW91 and PBE values. It is also rather surprising to find that the performance of the RPBE potential is the worst among considered GGA functionals with a MAE of 4.56 pm. It is also worth pointing out that RPBE systematically tends to overestimate interatomic distances by 4.2 pm on average. Note again that the performance of the different exchange-correlation functionals examined in this work depends on the lattice type of a metal under consideration. For example, PBEsol produces more accurate interatomic distances of *fcc* metals while *bcc* and *hcp* metals are best described with PBE. Surprisingly, RPBE yields relatively accurate results for metals with the *bcc* lattice. See the Supporting Information for more details.

For the special cases of Mn, La, and Hg, the trends are similar, although the errors are larger than on the rest of transition metal cases. Indeed, RPBE provides the best description of Mn, although with an error of 9 pm. PBE almost reproduces the experimental value for La, whereas both CA and VWN underestimate it by 19 pm, and the rest of the functionals provide results within 2−12 pm. Finally, for Hg one finds that CA and VWN perform the best, with an error of 9 pm but overestimating the bond length, which is opposite to the behavior encountered in the rest of the metals.

3.B. Cohesive Energies. The accurate prediction of the cohesive energies of the whole transition metal series represents a stringent test for the different exchange-correlation functionals since it implies the breaking of all the different bonds depending on the crystal structure of a given element. Calculated E_{coh} values are displayed in Table 2 together with tabulated experimental data.[90] Results show that, as expected from the self-interaction error in the Coulomb contribution to the total energy, both CA and VWN implementation of LDA significantly overestimate the binding energy. In fact, these two functionals provide the worst results for a large fraction of the transition metal series. The mean absolute errors for CA and VWN on the 27 transition metals are 1.44 and 1.36 eV, respectively. The values corresponding to the standard GGA functionals (PW91 and PBE) represent a noteworthy improvement on the LDA values, expected from the more physically grounded nature of these exchange-correlation functionals. This is due, as commented above, to the fact that the electron density of transition metals largely deviates from that of simple metals which, in turn, is sufficiently well represented by the homogeneous electron gas model. Thus, PW91 and PBE provide, in general, the most accurate cohesive energies with a MAE of ∼0.34 eV and a MAPE of ∼8%. Finally, we consider the accuracy of RPBE and PBEsol functionals on predicting cohesive energies. Both functionals exhibit better behavior than LDA functionals, but none of them present any improvement

with respect to the GGA ones. This result is not unexpected for PBEsol since the restoration of the gradient expansion for slowly varying densities implies a poor description of exchange energies, vital to gaining good estimates of dissociation and cohesive energies.[47] The accuracy of RPBE and PBEsol is characterized by MAE values of 0.59 and 0.75 eV, respectively, which correspond both to a MAPE of ∼14%, almost doubling the MAPE exhibited by the other GGA functionals. Moreover, it is worth pointing out that, on average, RPBE tends to underestimate cohesive energies by 0.57 eV, whereas PBEsol overestimates them by 0.74 eV, in line with the trends in calculated interatomic distances discussed in the previous subsection. Nevertheless, one has to realize that for some metals, either RPBE (Sc, Ti, V, Mn, Fe, Co, Ni, Zr, and Ir) or PBEsol (Y, Nb, Mo, Ag, Cd, Au, and Hg) yields surprisingly good cohesive energies. This is an argument in favor of testing the accuracy of newly developed methods using a sufficiently large database of available experimental results.

It is noteworthy that, at variance with the situation concerning interatomic distance, the performance of the functionals here explored does not significantly depend on the type of crystal structure, clearly showing that the accuracies of PW91 and PBE functionals are especially good when computing the cohesive energy of metals, as shown in the Supporting Information. Only RPBE seems to be similarly adequate to PW91 and PBE for *bcc* metals. For the special cases of Mn, La, and Hg, the mean error is surprisingly small for some functionals and quite large for others. For instance, in the case of Mn, RPBE provides the best estimate with an error of 0.5 eV, and LDA errors are almost 100%. For La, the GGA functionals deviate only ∼0.1 eV from experimental values, while RPBE performs even worse than LDA. A different situation is found for Hg; here PBEsol provides the best description and PBE and PW91 the worst.

3.C. Bulk Moduli. Estimations of B_0 for the different metals under scope are listed in Table 3 together with the tabulated experimental data.[90] This is quite a difficult property, although, surprisingly, the error exhibited by all methods is similar to that corresponding to the cohesive energy. Hence, consistently with the situation already commented on for interatomic distances and cohesive energies, both LDA type functionals overestimate bulk moduli by a ME of ∼36 GPa, whereas, once again, the best performance is exhibited by the GGA functionals with ME values of 7.5 and 5.2 GPa for PW91 and PBE, respectively, although the MAE values are larger (∼16 GPa for both PW91 and PBE), indicating some sort of error compensation along the series. Here, the accuracy of RPBE is similar to that exhibited by PW91 and PBE and consistently better for *bcc* metals and somewhat worse for *fcc* metals, as detailed in the Supporting Information. However, it is interesting to point out that while PW91 and PBE systematically tend to overestimate this property, the RPBE functional exhibits an opposite behavior with a tendency to underestimate the bulk moduli of transition metals by 8 GPa, but with a MAE of 16 GPa. Finally, the PBEsol performance is closer to LDA and, therefore, worse than that of PW91 and PBE. In terms of MAPE, it is worth pointing out that PW91, PBE, and RPBE deviate from experiment by 10% and CA and VWN by 28%, and finally, PBEsol exhibits an intermediate behavior (18%).

Among the special cases (Mn, La, and Hg), Mn exhibits the largest deviations from experimental values with errors greater than 200 GPa regardless of the functional. On the contrary, in the case of La, all functionals are found to perform with a similar accuracy, although with errors below 6 GPa or ∼20%. Finally, in the case of Hg, LDA provides the best values, a behavior which has also been found for the cohesive energy and interatomic distances.

3.D. Surface Energies of Selected Metals. In this subsection, we investigate how the accuracy of a given functional in describing bulk properties affects surface energies, and ultimately, the magnitude of adsorption energy. Clearly, one has to restrict the study to a few metals and to the most stable surface only. Here, we choose to study the (111) surface of a set of transition metals with the common feature of exhibiting *fcc* crystal structure and for which experimental values are also available,[91] even if one must admit that accurate measurements of this property are extremely difficult. Nevertheless, note that the reported experimental error bars are below the significant figures here treated.[92] In addition, these are the metals commonly encountered in heterogeneous catalysts and, therefore, the ones for which the knowledge of this information appears to be most essential.

From the summary of results in Table 5, one can readily see that results obtained via linear regression of slab energies tend to be as accurate as those arising from the straightforward method involving bulk calculations. With respect to the accuracy of the different DFT methods explored in this work, the error analysis shows that all exchange-correlation functionals underestimate the surface energies with the exception of LDA for Cu and Ni. The lowest value of the MAE (0.2 J m^{-2}) corresponds to the LDA methods and is hardly consistent with the well-known tendency to overestimate bonding interactions. Naively, one would expect that an overestimated value of the cohesive energy results also in a larger value of the surface energy simply because the cost to create the surface will also be higher. GGA functionals exhibit a few times more pronounced deviations (MAEs) than the LDA methods. In fact, the MAPE values for LDA are ∼10%, whereas the GGA methods have a noticeable value of ∼35%. Interestingly, RPBE produces an even larger MAPE value of ∼45%, whereas here PBEsol presents the best performance among GGAs with a MAPE of roughly 20%. This finding is in line with the known anticorrelation between the accuracy of a GGA functional for the calculation of surface energies and adsorption energies, the case of the CO molecule adsorption being the typical example.[37,49] This can be easily understood from the following arguments: Methods overestimating/underestimating the bonding interactions such as LDA/GGA will predict larger/smaller surface energies simply because the cost to break a bond is larger/smaller. Consequently, the surface is less/more stable and tends to interact more/less with incoming adsorbates. This is likely to be the reason why RPBE provides CO adsorption energies which improve the PBE ones.[64] This trend on the surface energy is likely to be transferred to the energy profiles of surface reactions, affecting the thermodynamics and kinetics of a given process.[93,94]

CONCLUSIONS

Interatomic distances, cohesive energies, and bulk moduli of the three transition metal series (3d, 4d, and 5d) in the periodic table in their most stable crystal structures have been obtained using several exchange-correlation potentials. These are the CA and VWN implementation of LDA, the GGA type PW91 and PBE functionals, and the RPBE and PBEsol revisions of PBE. From the analysis of calculated results for these metals and from comparison to the available experimental data, it is

possible to obtain a rather complete picture concerning the performance of these functionals. This is done, however, by excluding the cases of Mn, La, and Hg, which for some or all properties present errors significantly larger than for the rest of the transition metals and bias the mean deviations. On the basis of the research scope, we present compelling evidence that (*i*) PW91 and PBE produce similar results for the majority of transition metals and yield the best overall accuracy for structural data, cohesive energies, and bulk moduli, as shown in Figure 2, based on MAPE. (*ii*) Except for a few elements, LDA yields less accurate interatomic distances, cohesive energies, and bulk moduli than the typical GGA functionals. At the same time, as a consequence of the overestimation of bond interactions, LDA does not underestimate the surface energies so strongly as the other considered functionals. (*iii*) PBEsol, designed to yield good results for lattice parameters of solids, improves it over PBE only for six transition metals, while its performance for 14 other bulks is clearly inferior to those of PW91 or PBE. In general, PBEsol appears to exhibit a performance in between that of GGA and LDA. In this sense, it overestimates binding energies more than PBE or PW91 but less than LDA. (*iv*) The overall performance of RPBE for lattice parameters, cohesive, and surface energies of transition metals is worse than that of PW91 and PBE, although results for bulk moduli are of comparable quality. The better performance of RPBE in describing chemisorption energies seems to result from a severe underestimation of cohesive energies, and consequently, an overestimation of the surface stability, which hinders its chemical activity. (*v*) The bulk crystal structure seems to be a factor to take into account when using a given functional and certain properties. Cohesive energies seem to be unaffected by the type of crystal structure, although interatomic distances of *fcc* are better reproduced with PBEsol, and *bcc* and *hcp* interatomic distances are better reproduced by GGA and RPBE functionals, respectively. Concerning bulk moduli, RPBE is especially good when describing the bulk moduli of *hcp* and *bcc* solids.

Finally, even if among the explored exchange-correlation potentials the average performance of PBE results to be the best, one must be aware that non-negligible errors with respect to experimental results still remain. The origin of these errors has to be traced to approximations in the form of the exchange-correlation functional. On the one hand, it is likely that the *d* orbitals suffer from the self-interaction error as is the case in transition metal oxides and also in *f* orbitals in rare earth elements and their oxides. In principle, this can be remedied through self-interaction corrected DFT methods.[95] A second source of error, especially for the heavier transition metal elements, is the lack of explicit nonscalar relativistic effects such as spin−orbit interactions. Nevertheless, the precise contribution of these effects remains an open question.

To summarize, whereas PW91 and PBE functionals represent a significant improvement over the LDA type functional, the RPBE and PBEsol do not necessarily improve over either PW91 or PBE and should be used with caution because improvement in some property is at the cost of worsening the description of others. Likewise, one must insist that because of the peculiarities and particular chemistry of each transition metal element, it is advisable to test the performance of newly developed functionals for the whole series rather than concentrating on a few cases only.

■ ASSOCIATED CONTENT

Supporting Information

Figure S1 shows schematic representations of the lattice structures discussed in the work. Tables S1−S3 display interatomic distances, cohesive energies, and bulk moduli, respectively, analogous to Tables 1−3 but including CA and PW91 results. Tables S4−S6 include an error analysis analogous to that of Table 4 but carried out exclusively for *fcc*, *bcc*, or *hcp* metals. Table S7 contains atomic configuration and atomic energy reference data. This information is available free of charge via the Internet at http://pubs.acs.org/.

■ AUTHOR INFORMATION

Corresponding Author

*E-mail: francesc.illas@ub.edu.

Notes

The authors declare no competing financial interest.

■ ACKNOWLEDGMENTS

This work was supported by the Spanish MICINN FIS2008-02238 and MINCECO CTQ2012-30751 grants, *Generalitat de Catalunya* (grants 2009SGR1041 and XRQTC), and, in part, by grants from the National Science and Technology Development Agency (NSTDA Chair Professor and NANOTEC Center for the Design of Nanoscale Materials for Green Nanotechnology), the Kasetsart University Research and Development Institute (KURDI), the Commission on Higher Education, Ministry of Education ("the National Research University Project of Thailand (NRU)" and "Postgraduate Education and Research Programs in Petroleum and Petrochemicals and Advanced Materials"). P.J. would like to thank the Office of the Higher Education Commission, Thailand for supporting him with a grant under the program Strategic Scholarships for Frontier Research Network for the Ph.D. Program Thai Doctoral degree and the Graduate School of Kasetsart University for his research. F.V. thanks the Spanish MICINN for the postdoctoral grant under the program *Juan de la Cierva* (JCI-2010-06372). S.M.K. is grateful to the Spanish *Ministerio de Educación, Cultura y Deporte* for the predoctoral FPU Grant AP2009-3379, and F.I. acknowledges additional support through the ICREA Academia award for excellence in research.

■ REFERENCES

(1) Parr, R. G.; Yang, W. *Density Functional Theory of Atoms and Molecules*; Oxford University Press: Oxford, U. K., 1989.
(2) McWeeny, R. *Methods of Molecular Quantum Mechanics*; Academic Press: London, U. K., 1992.
(3) Cramer, C. J.; Truhlar, D. G. *Phys. Chem. Chem. Phys.* **2009**, *11*, 10757.
(4) Payne, M. C.; Teter, M. P.; Allan, D. C.; Arias, T. A.; Joannopolos, J. D. *Rev. Mod. Phys.* **1992**, *64*, 1045−1097.
(5) Huang, P.; Carter, E. A. *Annu. Rev. Phys. Chem.* **2008**, *59*, 261.
(6) van Santen, R. A.; Neurock, M. *Molecular Heterogeneous Catalysis*; Wiley-VCH: Weinheim, Germany, 2006.
(7) Valiev, M.; Bylaska, E. J.; Govind, N.; Kowalski, K.; Straatsma, T. P.; Van Dam, H. J. J.; Wang, D.; Nieplocha, J.; Apra, E.; Windus, T. L.; de Jong, W. *Comput. Phys. Commun.* **2010**, *181*, 1477−1489.
(8) Iwata, J. I.; Takahashi, D.; Oshiyama, A.; Boku, T.; Shiraishi, K.; Okada, S.; Yabana, K. *J. Comput. Phys.* **2010**, *229*, 2339−2363.
(9) Cohen, A. J.; Mori-Sanchez, P.; Yang, W. *Chem. Rev.* **2012**, *112*, 289.
(10) Yang, K.; Zheng, J. J.; Zhao, Y.; Truhlar, D. G. *J. Chem. Phys.* **2010**, *132*, 164117.

(11) Zhao, Y.; Truhlar, D. G. *Theor. Chem. Acc.* **2008**, *120*, 215−241.
(12) Boese, A. D.; Martin, J. M. L. *J. Chem. Phys.* **2004**, *121*, 3405−3416.
(13) Becke, A. D. *J. Chem. Phys.* **1993**, *98*, 5648−5652.
(14) Peverati, R.; Truhlar, D. G. *Phys. Chem. Chem. Phys.* **2012**, *14*, 13171−13174.
(15) Adamo, C.; Barone, V. *J. Chem. Phys.* **1999**, *110*, 6158.
(16) Vydrov, O. A.; Scuseria, G. E. *J. Chem. Phys.* **2006**, *125*, 234109.
(17) (a) Heyd, J.; Scuseria, G. E.; Ernzernhof, M. *J. Chem. Phys.* **2003**, *518*, 8207;(b) *ibid.* **2006**, *124*, 219906(E).
(18) Moreira, I. de P. R.; Illas, F.; Martin, R. L. *Phys. Rev. B* **2002**, *65*, 155102.
(19) Feng, X. B.; Harrison, N. M. *Phys. Rev. B* **2004**, *69*, 035114.
(20) Bredow, T.; Gerson, A. R. *Phys. Rev. B* **2000**, *61*, 5194.
(21) Muscat, J.; Wander, A.; Harrison, N. M. *Chem. Phys. Lett.* **2001**, *342*, 397.
(22) Kudin, K. N.; Scuseria, G. E.; Martin, R. L. *Phys. Rev. Lett.* **2002**, *89*, 266402.
(23) Muñoz, D.; Harrison, N. M.; Illas, F. *Phys. Rev. B* **2004**, *69*, 085115.
(24) Perry, J. K.; Tahir-Kheli, J.; Goddard, W. A. *Phys. Rev. B* **2001**, *63*, 144510.
(25) Feng, X.; Harrison, N. M. *Phys. Rev. B* **2004**, *70*, 092402.
(26) Moreira, I. de P. R.; Dovesi, R. *Int. J. Quantum Chem.* **2004**, *99*, 811.
(27) Paier, J.; Marsman, M.; Kresse, G. *J. Chem. Phys.* **2007**, *127*, 024103.
(28) Tran, F.; Koller, D.; Blaha, P. *Phys. Rev. B* **2012**, *86*, 134406.
(29) Zhao, Y.; Truhlar, D. G. *Acc. Chem. Res.* **2008**, *41*, 157−167.
(30) Luo, S.; Zhao, Y.; Truhlar, D. G. *J. Phys. Chem. Lett.* **2012**, *3*, 2975−2979.
(31) Ruzsinszky, A.; Sun, J.; Xiao, B.; Csonka, G. I. *J. Chem. Theory Comput.* **2012**, *8*, 2078−2087.
(32) Hao, P.; Fang, Y.; Sun, J.; Csonka, G. I.; Philipsen, P. H. T.; Perdew, J. P. *Phys. Rev. B* **2012**, *85*, 014111.
(33) Sun, J.; Marsman, M.; Csonka, G. I.; Ruzsinszky, A.; Hao, P.; Kim, Y.-S.; Kresse, G.; Perdew, J. P. *Phys. Rev. B* **2011**, *84*, 035117.
(34) Schimka, L.; Harl, J.; Kresse, G. *J. Chem. Phys.* **2011**, *134*, 024116.
(35) Sun, J.; Marsman, M.; Ruzsinszky, A.; Kresse, G.; Perdew, J. P. *Phys. Rev. B* **2011**, *83*, 121410.
(36) Haas, P.; Tran, F.; Blaha, P.; Schwarz, K. *Phys. Rev. B* **2011**, *83*, 205117.
(37) Schimka, L.; Harl, J.; Stroppa, A.; Grüneis, A.; Marsman, M.; Mittendorfer, F.; Kresse, G. *Nat. Mater.* **2010**, *9*, 741−744.
(38) Harl, J.; Schimka, L.; Kresse, G. *Phys. Rev. B* **2010**, *81*, 115126.
(39) Haas, P.; Tran, F.; Blaha, P.; Pedroza, L. S.; da Silva, A. J. R.; Odashima, M. M.; Capelle, K. *Phys. Rev. B* **2010**, *81*, 125136.
(40) Harl, J.; Kresse, G. *Phys. Rev. Lett.* **2009**, *103*, 056401.
(41) Perdew, J. P.; Ruzsinszky, A.; Csonka, G. I.; Constantin, L. A.; Sun, J. *Phys. Rev. Lett.* **2009**, *103*, 026403.
(42) Haas, P.; Tran, F.; Blaha, P. *Phys. Rev. B* **2009**, *79*, 085104.
(43) Ruzsinszky, A.; Csonka, G. I.; Scuseria, G. E. *J. Chem. Theory Comput.* **2009**, *5*, 763−769.
(44) Csonka, G. I.; Perdew, J. P.; Ruzsinszky, A.; Philipsen, P. H. T.; Lebègue, S.; Paier, J.; Vydrov, O. A.; Ángyán, J. G. *Phys. Rev. B* **2009**, *79*, 155107.
(45) Perdew, J. P.; Ruzsinszky, A.; Csonka, G. I.; Vydrov, O. A.; Scuseria, G. E.; Constantin, L. A.; Zhou, Z.; Burke, K. *Phys. Rev. Lett.* **2008**, *101*, 239702.
(46) Marsman, M.; Paier, J.; Stroppa, A.; Kresse, G. *J. Phys.: Condens. Matter* **2008**, *20*, 064201.
(47) Perdew, J. P.; Ruzsinszky, A.; Csonka, G. I.; Vydrov, O. A.; Scuseria, G. E.; Constantin, L. A.; Zhou, X.; Burke, K. *Phys. Rev. Lett.* **2008**, *100*, 136406.
(48) Zhao, Y.; Truhlar, D. G. *J. Chem. Phys.* **2008**, *128*, 184109.
(49) Stroppa, A.; Kresse, G. *New J. Phys.* **2008**, *10*, 063020.
(50) Ropo, M.; Kokko, K.; Vitos, L. *Phys. Rev. B* **2008**, *77*, 195445.
(51) Mattsson, A. E.; Armiento, R.; Paier, J.; Kresse, G.; Wills, J. M.; Mattsson, T. R. J. *Chem. Phys.* **2008**, *128*, 084714.
(52) Madsen, G. K. *Phys. Rev. B* **2007**, *75*, 195108.
(53) Tran, F.; Laskowski, R.; Blaha, P.; Schwarz, K. *Phys. Rev. B* **2007**, *75*, 115131.
(54) Wu, Z.; Cohen, R. E. *Phys. Rev. B* **2006**, *73*, 235116.
(55) Paier, J.; Marsman, M.; Hummer, K.; Kresse, G.; Gerber, I. C.; Ángyán, J. G. J. *Chem. Phys.* **2006**, *124*, 154709.
(56) Gajdo, M.; Eichler, A.; Hafner, J. *J. Phys.: Condens. Matter* **2004**, *16*, 1141−1164.
(57) Staroverov, V. N.; Scuseria, G. E.; Tao, J.; Perdew, J. P. *Phys. Rev. B* **2004**, *69*, 075102.
(58) Kurth, S.; Perdew, J. P.; Blaha, P. *Int. J. Quantum Chem.* **1999**, *75*, 889−909.
(59) Grabowski, B.; Hickel, T.; Neugebauer, J. *Phys. Rev. B* **2007**, *76*, 024309.
(60) Ceperley, D. M.; Alder, B. J. *Phys. Rev. Lett.* **1980**, *45*, 566−569.
(61) Vosko, S. H.; Wilk, L.; Nusair, M. *Can. J. Phys.* **1980**, *58*, 1200−1211.
(62) Perdew, J. P.; Wang, Y. *Phys. Rev. B* **1992**, *45*, 13244−13249.
(63) Perdew, J. P.; Burke, K.; Ernzerhof, M. *Phys. Rev. Lett.* **1996**, *77*, 3865−3868.
(64) Hammer, B.; Hansen, L. B.; Nørskov, J. K. *Phys. Rev. B* **1999**, *59*, 7413−7421.
(65) Kresse, G.; Furthmuller, J. *Phys. Rev. B* **1996**, *54*, 11169−11186.
(66) Blöchl, P. E.; Jepsen, O.; Andersen, O. K. *Phys. Rev. B* **1994**, *49*, 16223−16233.
(67) Blöchl, P. E. *Phys. Rev. B* **1994**, *50*, 17953−17979.
(68) Monkhorst, H. J.; Pack, J. D. *Phys. Rev. B* **1976**, *13*, 5188−5192.
(69) Viñes, F.; Sousa, C.; Liu, P.; Rodriguez, J. A.; Illas, F. *J. Chem. Phys.* **2005**, *122*, 174709.
(70) Boettger, J. C. *Phys. Rev. B* **1994**, *49*, 16798−16800.
(71) Kozlov, S. M.; Viñes, F.; Nilius, N.; Shaikhutdinov, S.; Neyman, K. M. *J. Phys. Chem. Lett.* **2012**, *3*, 1956−1961.
(72) Da Silva, J. L. F.; Stampfl, C.; Scheffler, M. *Surf. Sci.* **2006**, *600*, 703−715.
(73) Gražulis, S.; Chateigner, D.; Downs, R. T.; Yokochi, A. T.; Quiros, M.; Lutterotti, L.; Manakova, E.; Butkus, J.; Moeck, P.; Le Bail, A. *J. Appl. Crystallogr.* **2009**, *42*, 726−729.
(74) Saw, C. K.; Beaudry, B. J.; Stassis, C. *Phys. Rev. B* **1983**, *27*, 7013−7017.
(75) Wyckoff, R. W. G. *Crystal Structures*, 2nd ed.; Interscience Publishers: New York, 1963; pp 7−83.
(76) Smura, C. F.; Parker, D. R.; Zbiri, M.; Johnson, M. R.; Gál, Z. A.; Clarke, S. J. *J. Am. Chem. Soc.* **2011**, *133*, 2691−2705.
(77) Bradley, A. J.; Thewlis, J. *Proc. R. Soc. London, Ser. A* **1927**, *115*, 456−471.
(78) Neale, J. W.; Walker, A. M.; Marshall, W. G.; Tucker, M. G.; Francis, D. J.; Stone, H. J.; McCammon, C. A. *J. Appl. Crystallogr.* **2008**, *41*, 886−896.
(79) Jørgensen, J.-E.; Smith, R. I. *Acta Crystallogr., Sect. B* **2006**, *62*, 987−992.
(80) Ling, C. D.; Avdeev, M.; Kharton, V. V.; Yaremchenko, A. A.; Macquart, R. B.; Hoelzel, M. *Chem. Mater.* **2010**, *22*, 532−540.
(81) Bernuy-Lopez, C.; Allix, M.; Bridges, C. A.; Claridge, J. B.; Rosseinsky, M. J. *Chem. Mater.* **2007**, *19*, 1035−1043.
(82) Kittel, C. *Introduction to Solid State Physics*, 8th ed.; John Wiley & Sons: New York, 2005; p 20.
(83) Moshopoulou, E. G.; Ibberson, R. M.; Sarrao, J. L.; Thompson, J. D.; Fisk, Z. *Acta Crystallogr., Sect. B* **2006**, *62*, 173−189.
(84) Ellner, M. *J. Less-Common Met.* **1981**, *78*, 21−32.
(85) Suh, I.-K.; Ohta, H.; Waseda, Y. *J. Mater. Sci.* **1988**, *23*, 757−760.
(86) Dubrovinsky, L. S.; Saxena, S. K. *Phys. Chem. Miner.* **1997**, *24*, 547−550.
(87) Koichi, S.; Taku, T.; Shigeaki, S. *Acta Crystallogr., Sect. B* **2003**, *59*, 701−708.
(88) Davey, W. P. *Phys. Rev.* **1925**, *25*, 753−761.

(89) Görling, A.; Trickey, S. B.; Gisdakis, P.; Rösch, N. In *Topics in Organometallic Chemistry*; Brown, J., Hofmann, P., Eds.; Springer: Heidelberg, Germany, 1999; Vol. *4*, pp 109−163.
(90) Young, D. A. *Phase Diagrams of the Elements*; University of California Press: Berkeley, CA, 1991; pp 273−381.
(91) de Boer, F. R.; Boom, R.; Mattens, W. C. M.; Miedama, A. R.; Niessen, A. K. *Cohesion in Metals*; North-Holland: Amsterdam, 1988.
(92) Tyson, W. R.; Miller, W. A. *Surf. Sci.* **1977**, *62*, 267−276.
(93) Fajin, J. L. C.; Illas, F.; Gomes, J. R. B. *J. Chem. Phys.* **2009**, *130*, 224702.
(94) Roldán, A.; Ricart, J. M.; Illas, F. *Theor. Chem. Acc.* **2009**, *123*, 119−126.
(95) Svane, A. *Phys. Rev. B* **1996**, *53*, 4275−4286.